Available online at www.sciencedirect.com
ScienceDirect
Mathematics and Computers in Simulation 76 (2007) 94–98
MATHEMATICS AND COMPUTERS IN SIMULATION
www.elsevier.com/locate/matcom

A nonuniform mesh semi-implicit CE–SE method modelling unsteady flow in tapered ducts

S. Jerez, J.V. Romero*, M.D. Roselló, J.M. Arnau

Instituto de Matemática Multidisciplinar, Universidad Politécnica de Valencia, Edificio 8G, 2°, P.O. Box 46022, Valencia, Spain

Available online 16 January 2007

Abstract

Recently, a semi-implicit one-dimensional CE–SE (conservation element–solution element) method for the calculation of the unsteady flow of one and several chemical species tracking in engine ducts has been developed in Arnau et al. [J.M. Arnau, S. Jerez, L. Jódar, J.V. Romero, A semi-implicit conservation element–solution element method for chemical species transport simulation to tapered ducts of internal combustion engine, Math. Comput. Simul. 73 (1/4) (2006) 28–37]. This new scheme improves the accuracy of the original CE–SE with a similar computational cost. In this paper, we modify the semi-implicit CE–SE method taking a nonuniform discretization of the space–time domain. The mesh is constructed by considering the geometrical characteristics of the tapered ducts, which are composed of constant and conical sections. The goal is to reduce the computational cost and to increase the accuracy of the approximated solution. Numerical results of the semi-implicit CE–SE for uniform and nonuniform meshes are compared with experimental data.

Keywords: CE–SE scheme; Semi-implicit method; Nonuniform mesh; Nonlinear system; Tapered ducts

1. Introduction

The numerical simulation of wave dynamics represents an essential tool in the design and optimization of new internal combustion engines. Lately, the use of one-dimensional gas dynamic models in the automotive industry has notably increased since great part of the experimental tests of the validation stage is reduced. The behavior of an unsteady one-dimensional flow of a perfect gas in a tapered duct with friction and heat transfer is modelled by the following nonlinear hyperbolic system of partial differential equations [5]

$$\begin{cases} W_t + F_x(W) + S(W) = 0, \quad x \in [b_1, b_2] \subset \mathbb{R}, \quad 0 < t \le T < +\infty \\ W(x,0) = W_0(x), \quad W(b_1,t) = H(t), \quad W(b_2,t) = G(t) \end{cases} \tag{1}$$

where W is the vector of variables (density, momentum and total energy), $F(W)$ the flux vector and $S(W)$ represents the terms concerning to the variation of section of the duct, friction and heat transfer.

In spite of the fact that some works have been published relating to the analytical solution of the governing equation system (1), usually it can only be solved by means of numerical methods. This fact has given rise to search of new and better numerical methods in terms of reliability, accuracy, robustness and computational cost.

* Corresponding author.
E-mail addresses: sjerez@imm.upv.es (S. Jerez), jvromero@imm.upv.es (J.V. Romero), drosello@imm.upv.es (M.D. Roselló), jmaarnau@imm.upv.es (J.M. Arnau).

0378-4754/$32.00 © 2007 IMACS. Published by Elsevier B.V. All rights reserved.
doi:10.1016/j.matcom.2007.01.002

Comparative studies of computational cost and accuracy of numerical methods modelling the behavior of unsteady flows are presented in [6]. In these studies, the CE–SE method is an accurate algorithm with low computational cost for problems involving discontinuities, such as shock waves, contact surfaces and their mutual interactions [4] in ducts with constant cross section. The CE–SE scheme uses the integral and differential forms of the system in the space–time domain for calculating the numerical solution [2] and it's free of any artificial stabilization mechanism. When the flux flows through ducts of variable section, this explicit method generates a fictional value in mass flow [5].

Recently, we have developed a semi-implicit CE–SE method with the main goal to improve the numerical results of the original CE–SE in ducts with variable cross section area [5]. This scheme gives a better discretization of the source term. Besides, our semi-implicit method has been adapted to the calculation of chemical species tracking, obtaining highly accurate numerical solutions [1].

In this paper, we modify our semi-implicit CE–SE method to make use of nonuniform discretizations of the space–time domain. The goal is to reduce the computational cost and to improve the accuracy of the numerical solution of the semi-explicit CE–SE scheme. Also, we present an example under real conditions. In this example, the ducts are composed of constant and conical sections, which implies the presence of nonsmooth changes of the derivative of the area. The mesh is constructed by decreasing spatial step in the duct parts with variable area and increasing spatial step in the constant sections. We compare the numerical results of the mass flow and pressure variables of the semi-implicit CE–SE scheme for uniform and nonuniform meshes.

2. Semi-implicit CE–SE method for nonuniform meshes

In this section, the semi-implicit CE–SE method [5] is adapted to a nonuniform spatial mesh. In each step of time, n, we take a fixed temporal step, $(\Delta t)_n$, and we calculate the lesser spatial step, $(\Delta x)_{\min}$, verifying the necessary condition for the stability of the CE–SE method [3], the *CFL condition*, $[\max_{x\in[b_1,b_2]}(|u|+|a|)](\Delta t)_n/(\Delta x)_{\min} \le 1$, where u is the flux velocity and a is the sound speed.

The semi-implicit CE–SE method [5] divides the space–time domain into solution elements (SE), nonoverlapping regular rhombus given by dashed lines, where the numerical approximation is a simple linear function of space and time evaluated in the center of the rhombus, and conservation elements (CE), nonoverlapping rectangles given by solid lines where the integral form of the system (1) is required.

In a nonuniform discretization, two types of nodes are considered, see Fig. 1. The *grid points*, x_j, represented by $\{\bullet\}$, are generated as $x_j = x_{j-1/2} + (\Delta x)_j$, with $(\Delta x)_j \ge (\Delta x)_{\min}$. The *solution points*, x'_j, represented by $\{\circ\}$, are calculated as $x'_j = (x_{j-1/2} + x_{j+1/2})/2$ in the internal points and $x'_j = x_j$ in the boundary nodes. The grid points describe the division of the domain in rectangles and the numerical solution is calculated in the solution points.

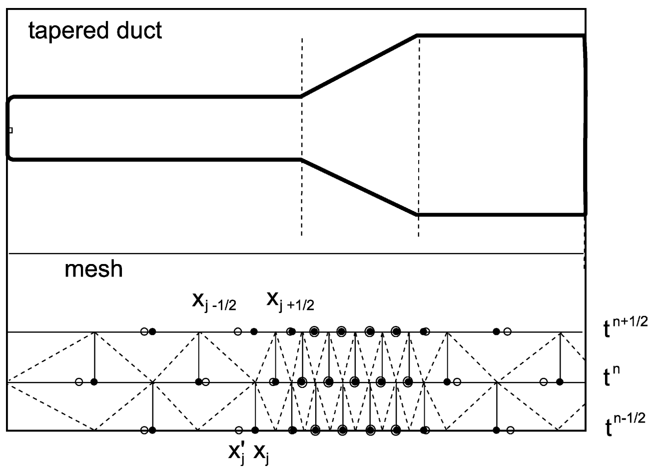

Fig. 1. Spatial nonuniform mesh.

In each solution element, SE(j, n), each component of the solution $W(x, t) = [w_1, w_2, w_3]$ is approximated by means of first order Taylor expansion in (x'_j, t^n),

$$\tilde{\omega}_k(x, t; j, n) = (\sigma_k)_j^n + (\alpha_k)_j^n(x - x'_j) + (\beta_k)_j^n(t - t^n), \quad k = 1, 2, 3. \tag{2}$$

We denote the approximation of F and S by $\tilde{F}$ and $\tilde{S}$. $\tilde{F}$ is the first order Taylor expansion of $F(\tilde{W})$ and $\tilde{S}(x, t; j, n) = S(\tilde{W}(x'_j, t^{n+1/2}; j, n))$. With this approximation, the solution is described by $(\sigma_k)_j^n, (\alpha_k)_j^n, (\beta_k)_j^n$. If the coefficients in the step n are known, we are going to compute them in the step $n + 1/2$. In each CE, we calculate $(\sigma_k)_j^{n+1/2}$ using the integral form of (1),

$$\iint_{\mathrm{CE}(j,n+1/2)} \left(\frac{\partial \tilde{\omega}_k}{\partial t} + \frac{\partial \tilde{f}_k}{\partial x}\right) \mathrm{d}x\,\mathrm{d}t + \iint_{\mathrm{CE}(j,n+1/2)} \tilde{s}_k \,\mathrm{d}x\,\mathrm{d}t = 0, \qquad k = 1, 2, 3. \tag{3}$$

Applying the Green's Theorem to the first integral of (3), and decomposing the second integral as the sum of three integrals defined in each rhombus SE into of the rectangle CE($j; n + 1/2$), we obtain

$$\begin{aligned}
(\sigma_k)_j^{n+1/2}(\Delta x) + \frac{(\Delta x)(\Delta t)}{4}(\tilde{s}_k)_j^{n+1/2} &= (\Delta x)_+ \left((\sigma_k)_{j+1/2}^n - \frac{\Delta t}{4}(\tilde{s}_k)_{j+1/2}^n\right) \\
&\quad + (\Delta x)_- \left((\sigma_k)_{j-1/2}^n - \frac{\Delta t}{4}(\tilde{s}_k)_{j-1/2}^n\right) + (\alpha_k)_{j-1/2}^n \left(\frac{(x_j - x'_{j-1/2})^2}{2} - \frac{(x_{j-1/2} - x'_{j-1/2})^2}{2}\right) \\
&\quad + (\alpha_k)_{j+1/2}^n \left(\frac{(x_{j+1/2} - x'_{j+1/2})^2}{2} - \frac{(x_j - x'_{j+1/2})^2}{2}\right) \\
&\quad - [g_k(x, t; j + 1/2, n) - g_k(x, t; j - 1/2, n)],
\end{aligned} \tag{4}$$

where $g_k(x, t; \cdot, \cdot)$, $(\tilde{s}_k) := \tilde{s}_k(\cdot, \cdot)$, $k = 1, 2, 3$, are defined in [5] and $\Delta x = x_{j+1/2} - x_{j-1/2}$, $(\Delta x)_+ = x_{j+1/2} - x_j$, $(\Delta x)_- = x_j - x_{j-1/2}$. Note that if the solution point is not $x'_j = (x_{j-1/2} + x_{j+1/2})/2$, it would appear the term $(\alpha_k)_j^{n+1/2}$ in (4) and it would have more unknowns than equations.

System (4) can be solved obtaining the second order equation with module

$$\frac{f_{\mathrm{r}}(\Delta t)}{2D_j}(\sigma_2)_j^{n+1/2}|(\sigma_2)_j^{n+1/2}| + \left(E_1 + \frac{(\Delta t)\delta_j}{4}E_2\right)(\sigma_2)_j^{n+1/2} = E_1E_2, \tag{5}$$

where the friction, f_{r}, is approximated as in [1] and E_k are obtained from (4) and do not depend on $(\sigma_k)_j^{n+1/2}$. Eq. (5) has real solution if

$$4\left|\frac{f_{\mathrm{r}}(\Delta t)}{2D_j}E_1E_2\right| \leq \left(E_1 + \frac{\Delta t}{4}\delta_j E_2\right)^2. \tag{6}$$

Inequality (6) is true when $E_1E_2 f_{\mathrm{r}} = 0$. In other case, Δt is chosen fulfilling

$$-\left(\frac{\Delta t}{4}\delta_j\right)^2 - \frac{(\Delta t)E_2E_1\delta_j}{2} + 2\left|\frac{f_{\mathrm{r}}(\Delta t)}{D_j}E_1E_2\right| \leq E_1^2. \tag{7}$$

Solving (6), we obtain up to four possible solutions. We choose one of them with the algorithm proposed in [5]. Once σ_2 is obtained, it is easy to calculate σ_1 and σ_3. Coefficients $(\alpha_k)_j^{n+1/2}$ and $(\beta_k)_j^{n+1/2}$ are calculated as in [5].

3. Numerical results

Some numerical tests have been carried out in order to evaluate the accuracy and the computational cost of the new method. An impulse test rig has been used to obtain the experimental data. In the upstream boundary condition, a pressure impulse has been imposed by means of the characteristics [6]. In the downstream boundary condition, an anechoic edge has been used. The geometrical characteristics of the duct are shown in Fig. 2.

Numerical results are shown in Figs. 3 and 4. We compare a uniform mesh with $\Delta x = 0.02$ m and three nonuniform meshes. The nonuniform meshes are constructed considering the characteristics of the ducts. In the constant parts, Δx

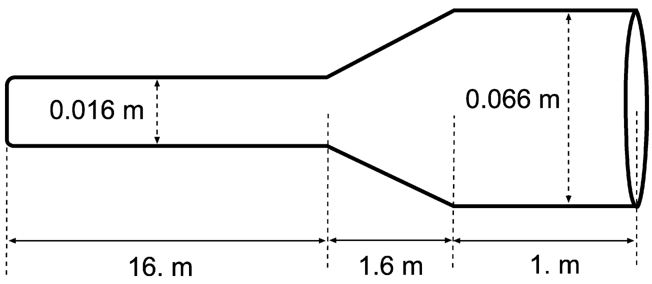

Fig. 2. Geometrical characteristics.

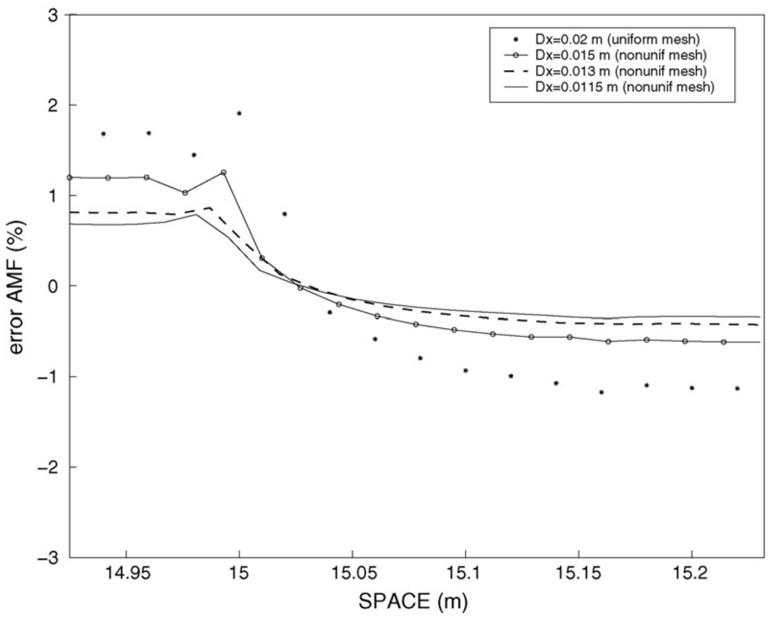

Fig. 3. Error AMF front MAMF for several $Dx:=(\Delta x)_{\text{con}}$ and $\Delta t = 0.0003$.

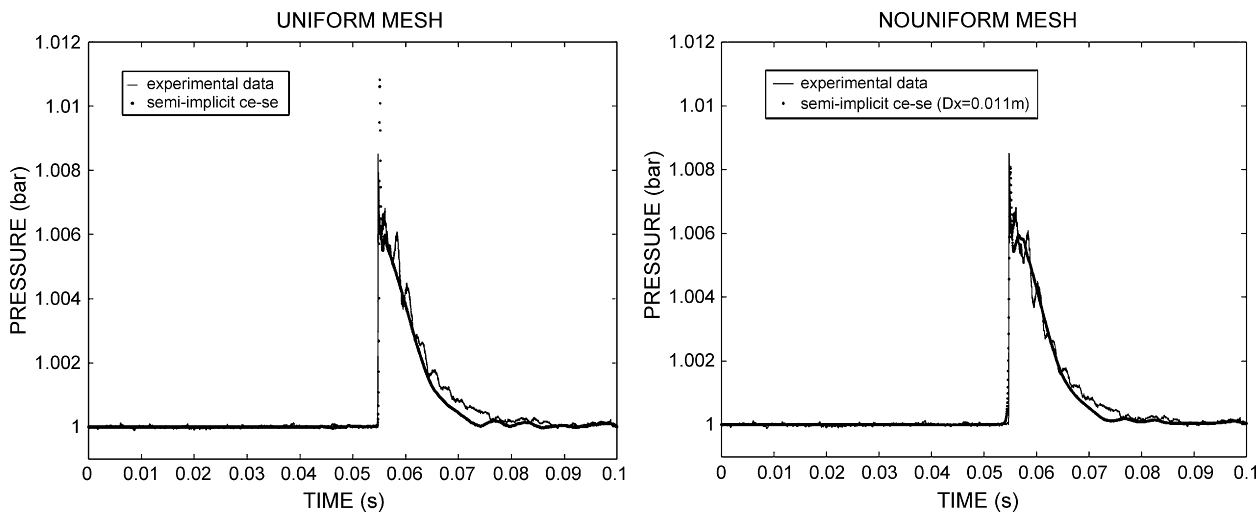

Fig. 4. Pressure profile after conical zone for $(\Delta x)_{\text{con}} = 0.0115$ and $\Delta t = 0.0003$.

is increased using $\Delta x = 0.025$ m and in the conical duct, we use $(\Delta x)_{con} = \{0.015, 0.013, 0.0115\}$ m. Fig. 3 represents the relative error of the air mass flow (AMF), it is, the difference between the AMF and the mean air mass flow (MAMF) [6]. We can see that the error decreases when we use nonuniform meshes with smaller $(\Delta x)_{con}$, since the mesh is refined in the conical zone.

In Fig. 4, we analyze the behavior of the pressure with an uniform mesh with $\Delta x = 0.02$ m and a nonuniform mesh with $(\Delta x)_{con} = 0.0115$ m in the conical zone. We compare the numerical results with experimental data. The results improve using the nonuniform mesh. Moreover, the computational cost is reduced approximately in a 25%, since we increase Δx in the constant zones.

Acknowledgements

This work has been supported by the Spanish M.E.C. and FEDER grants DPI2003-07153-C02-02 and DPI2004-08383-C03-03 and the Generalitat Valenciana.

References

[1] J.M. Arnau, S. Jerez, L. Jódar, J.V. Romero, A semi-implicit conservation element–solution element method for chemical species transport simulation to tapered ducts of internal combustion engine, Math. Comput. Simul. 73 (1/4) (2006) 28–37.

[2] G. Briz, P. Giannattasio, Applicazione dello Schema Numerico Conservation Element–Solution Element al Calcolo del Flusso Intazionario nei Condotti dei Motori a C.I., in: Proceedings of the 48th ATI National Congress, Taomina, Italy, 1993, pp. 233–247.

[3] S.C. Chang, The method of space–time conservation element and solution element—a new approach for solving the Navier–Stokes and Euler equations, J. Comput. Phys. 119 (1995) 295–324.

[4] S.C. Chang, X.Y. Wang, C.Y. Chow, The space–time conservation element and solution element method—a new high-resolution and genuinely multidimensional paradigm for solving conservation laws, J. Comput. Phys. 156 (1999) 89–136.

[5] S. Jerez, J.V. Romero, M.D. Roselló, F.J. Arnau, A semi-implicit space–time CE–SE method to improve mass conservation through tapered ducts in internal combustion engines, Math. Comput. Model. 40 (9/10) (2004) 941–951.

[6] F. Payri, J. Galindo, J.R. Serrano, F.J. Arnau, Analysis of numerical methods to solve one-dimensional fluid-dynamic governing equations under impulsive flow in tapered ducts, Int. J. Mech. Sci. 46 (7) (2004) 981–1004.